

ESTIMATION OF THE COUPLING IMPEDANCE FOR THE SPring-8 STORAGE RING

T. Yoshiyuki, T. Kusaka, M. Hara, and S. H. Be
RIKEN-JAERI Synchrotron Radiation Facility Design Team
2-28-8 Honkomagome, Bunkyo-ku, Tokyo 113, Japan

Abstract

The coupling impedance of vacuum chamber components is estimated for the SPring-8 storage ring. Three different approaches are discussed; analytical calculation, numerical simulation, and measurement. The results turn out that the contribution to the impedance is mainly attributed to RF cavities, bellows, flanges, and transitions to ID chambers.

Introduction

The SPring-8 storage ring is under design to be a low emittance synchrotron-radiation ring covering even the hard x-ray domain. High brilliance, which is implied by the low emittance, is related to large stored beam current in the ring. The beam current is, however, limited by the coherent instabilities of bunched beam. The important ingredients to evaluate the instabilities are a longitudinal coupling impedance Z/n , and a transverse impedance Z_{\perp} , the latter of which is usually correlated to the former. The storage ring consists of a large variety of structures which contribute to the impedance: vacuum chambers, bellows, gaps between flanges, step changes, box-like objects, vacuum ports, slits of RF contacts, RF cavities, and so on. Charged particles passing through the above components induce electromagnetic fields that act back on the beam, which results in energy losses and instabilities. The impedance is usually employed to describe the interaction of the beam with the environment. In order to estimate the effect on the beam more precisely, a detailed impedance analysis is carried out. In this report, we analyze the contribution of several vacuum components to the impedance, and suggest the way to minimize the energy losses.

Motivation of impedance estimate

Before a quantitative estimation of the impedance, we must get a reasonable idea on how much it can be allowed. The allowable impedance $|Z/n|$ is, in a classical stability criterion,¹ described by

$$\left| \frac{Z}{n} \right| \leq \frac{\alpha E}{c I_p} \left(\frac{\Delta E}{E} \right)^2, \quad (1)$$

where α is the momentum compaction factor, E the total particle energy, $\Delta E/E$ the FWHM of relative energy distribution, and I_p the peak current defined by

$$I_p = I_{AV} \frac{2\pi R}{3M\sigma_1} \quad (2)$$

I_{AV} is the average current in M bunches, σ_1 the rms bunch length, and $2\pi R$ the circumference of the ring. n is the ratio of storage ring circumference to the wavelength of perturbation traveling around the bunch. For our storage ring; $E = 8$ GeV, $\alpha = 1.5 \times 10^{-4}$, $\Delta E/E = 3 \times 10^{-3}$, $I_{AV} = 100$ mA, $2\pi R = 1,436$ m, $M = 1000$, and $\sigma_1 = 3.2$ mm, therefore $|Z/n| < 0.7 \Omega$. This quantity is relatively small compared with the other rings,² indicating that the impedance problem is more serious in our ring.

Method of impedance estimate

Since an exact analysis of the impedance of a storage ring is impossible, some different approaches have been developed to estimate this quantity;

- analytical calculations for several simple geometries,
- numerical simulations of electromagnetic fields in some elements of the vacuum chamber, and
- impedance measurements for test components.

We can obtain the contribution of several simple geometries to the longitudinal impedance analytically, assuming a cylindrical symmetry.² Naturally, it is followed that most of the vacuum components can not be evaluated in this way owing to their complicated geometries.

The electromagnetic field, which is created by a bunch circulating through a given section of the vacuum chamber, can be computed numerically by means of TBCI³ and MAFIA.⁴ Either TBCI or MAFIA computes wake potentials as a function of delay with respect to the head of bunch, together with the loss parameters, when a Gaussian-distributed rigid bunch is traveling in structures. The results of numerical computations can be used for the longitudinal and transverse broad-band impedances, $Z_{\parallel}(\omega)$ and $Z_{\perp}(\omega)$, respectively, which are given by

$$Z_{\parallel}(\omega) = R_s \frac{1 + jQ \left(\frac{\omega_r - \omega}{\omega \omega_r} \right)}{1 + Q^2 \left(\frac{\omega_r - \omega}{\omega \omega_r} \right)^2} \quad Z_{\perp}(\omega) = R_s \frac{\omega_r}{\omega} \frac{1 + jQ \left(\frac{\omega_r - \omega}{\omega \omega_r} \right)}{1 + Q^2 \left(\frac{\omega_r - \omega}{\omega \omega_r} \right)^2}, \quad (3)$$

where R_s is the shunt impedance, Q the quality factor, and ω_r the resonant frequency ($= \omega_r/2\pi$). The loss parameters of different contributions are computed as a function of σ_1 , and summed for all the vacuum elements. The derivation of impedance is based on the fact that the loss parameter is proportional to the integral over the real part of impedance, according to

$$k_{\parallel}(\sigma_1) = \frac{1}{\pi} \int_0^{\infty} \text{Re}[Z_{\parallel}(\omega)] \cdot \exp\left(-\frac{\omega \sigma_1}{c}\right)^2 \cdot \omega \, d\omega \quad (4)$$

Therefore, the parameters of a broad-band impedance (f_r , Q , R_s) can be fitted to match a computed loss-parameter curve.⁵

On the other hand, the loss parameter can be measured for each element of the vacuum chamber by a coaxial wire method as discussed later. In principle every geometry can be measured in this method, but it is impossible to measure the loss parameters for all the kinds of elements of the storage ring. Practically, the loss parameters of most of the elements are acquired using both methods: numerical simulations and measurements.

Profile of vacuum chamber elements

The vacuum chamber is designed in a racetrack geometry of 8 cm wide and 4 cm high with a slot-isolated antechamber in which NEG strips are installed for pumping. Figure 1(a) shows the H-field lines for the first TM mode at a frequency of 4.3 GHz. Figure 1(b) also indicates deep penetration of electromagnetic

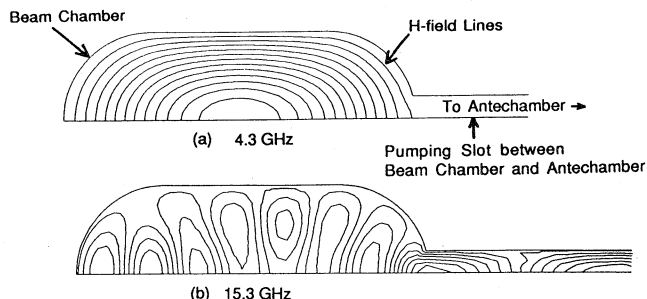


Fig. 1 Calculation of the H-fields lines for the vacuum chamber; (a) the first TM mode, 4.3 GHz, (b) higher-order mode, 15.3 GHz.

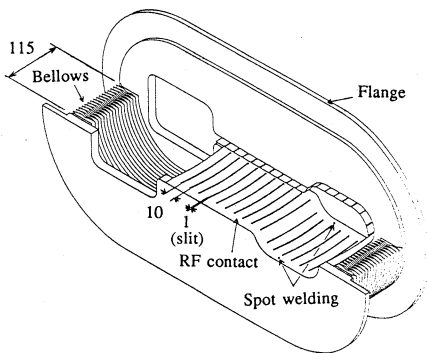


Fig. 2 RF contact by which the bellows are screened on the vacuum chamber.

fields into the pumping slot at frequencies above 15 GHz. A distortion of the H-field lines is remarkable compared with the beam chamber without antechamber. In case of a short bunch below 5 mm in length, as the modes above 15 GHz have a large contribution to the loss parameter according to Eq. (4), it may be that the slot has significant effects.

The RF contact screens the bellows to reduce the energy losses, and keep the electric contact between the chambers, as shown in Fig. 2. The numerous long and narrow slits absorb the shrinkage of bellows at baking, and make between the RF contact and bellows evacuated.

We adopt the Conflat flanges for our ring. The outer diameter gets over 350 mm in case of the connection between vacuum chambers. The gap between conventional Conflat flanges comes even to a few mm with a gasket inserted, but a special flange is designed so as to reduce the gap below 0.5 mm for a less impedance.

There is a radius discontinuity between the normal and insertion-device (ID) chamber. In fact, a tapered transition is used in place of a step change between different chambers. Nevertheless, the calculation was carried out assuming the step changes in the aspect of safety.

Calculation results

Analytical calculation

We have estimated the impedances of the various kinds of elements analytically: free space, space charge, resistive wall, bellows, flanges, pick-up electrodes, step changes, and slits and holes. Table 1 shows the impedances of typical elements. This preliminary study suggests that the bellows must be securely screened and RF contacts are effective to screen them. It also shows that transitions to ID chambers and flanges must be improved to achieve the design goal.

Table 1 Preliminary study of the impedance for analytical calculations

Impedance source	Number	$ Z/n $ (Ω)
Free space	—	0.2 ($f = 10$ GHz)
Space charge	—	4×10^{-6}
Resistive wall	—	0.1 ($f = 100$ MHz)
		0.01 ($f = 3.8$ GHz)
Bellows		
(without RF contact)	336	9.0
(with RF contact)	336	3.9×10^{-6}
Flanges (1 mm gap)	912	0.39
Step changes	96	0.26
Pick-up electrodes	432	0.05
Vacuum pump holes	~300	0.005

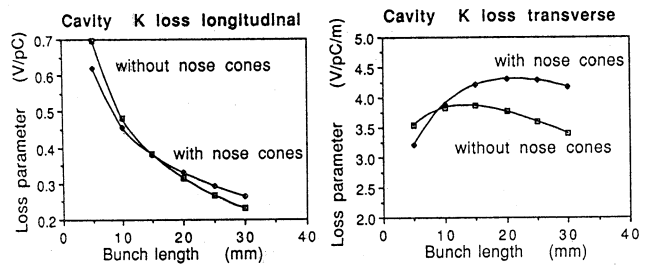


Fig. 3 Loss parameters for cavities both with and without nose cones; (a) longitudinal case, (b) transverse case.

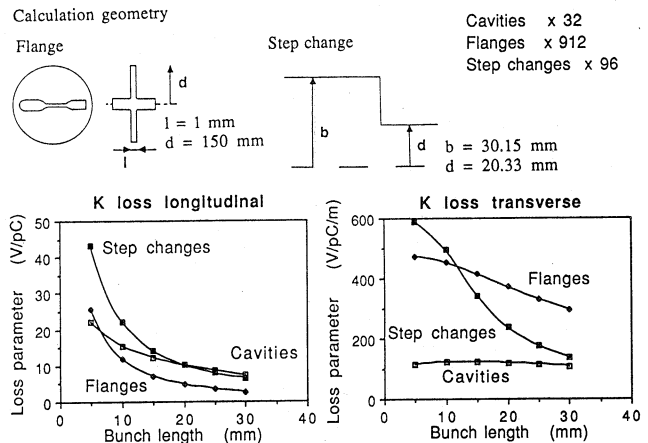


Fig. 4 Total loss parameters of the whole ring for typical components; (a) longitudinal case, (b) transverse case.

Numerical simulation

A 2D code, TBCI, is used to calculate the loss parameters, assuming again cylindrical symmetry. The simulation was carried out for longitudinal (monopole fields) and transverse impedance (dipole fields) independently, and applied to RF cavities, bellows, flanges, and transitions to ID chambers.

As far as RF cavities are concerned, the calculation has been done for the single-cell cavities both with nose cones, which have been already studied, and without nose cones, which are under design⁶ as a low impedance cavity for our ring. The loss parameters for both cases are plotted in Fig. 3 as a function of bunch length. We expected the loss parameters of the cavity without nose cones to be lower than those of the cavity with nose cones for every bunch length, but the loss parameters become reversed for short bunch lengths. The HOM impedances which have a harmful effect on the beam are suppressed in the cavity without nose cones as in Ref. 6, but the other HOM impedances seem to get larger than we expected, especially over cut-off frequency. In either case, it turns out that the contribution from the RF cavities to the loss parameter are inevitable.

Figure 4 shows the total loss parameters of the whole ring, considering only the elements which have large contributions to the impedance. The bellows themselves have large loss parameters, because the number is large ($N = 336$) and the shape looks like a pill-box type of cavity. On the other hand, once they are screened adequately by the RF contacts, the loss parameters are decreased tremendously even not to be plotted in Fig. 4. It turns out that in longitudinal case step changes have a large effect on the impedance, and step changes and flanges do in transverse one. However, as far as step changes are concerned, the loss parameters are, in fact, reduced further as the transitions to ID chambers get tapered. In case of flanges, the real loss parameters can be also reduced

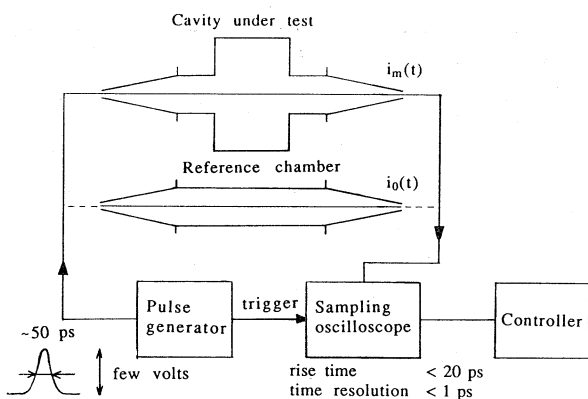


Fig. 5 Set-up for the measurement of the loss parameter.

at the rate of reduction of the gap, but they are still larger than those of the cavities in transverse case. The impedance needs to be decreased more.

In the next step, we calculate the loss parameters of the asymmetric geometries using the 3D code MAFIA. But as a 3D simulations have limitations such as the number of meshes, minimum bunch length, and computational time, there is some room for improvement.

Measurement of loss parameter

The coaxial wire method which has been described by Sands and Rees⁷ is a widely-spread tool for bench measurements of beam coupling impedance. By the introduction of a thin wire into the chamber components under test, a surface current distribution on the inner surface of the beam pipe can be obtained, which corresponds approximately to the current distribution produced by a passing bunch. When this image-current distribution has been perturbed by a discontinuity, a reaction on the wire takes place similar to that of a perturbed wake field on the bunch.

A measurement set-up is shown in Fig. 5. A nearly Gaussian pulse is generated with 50 ps of the minimum pulse width by a pulse generator. It travels through either the reference chamber with a thin wire at the axis of beam, or a component under test of the same mechanical length. Both signals, reference signal $i_0(t)$ and object signal $i_m(t)$, are recorded sequentially, and stored in a sampling oscilloscope which has time resolution below 1 ps. The data acquired into the oscilloscope are sent to a controller and then the longitudinal loss parameter $k_{//}(\sigma)$ is calculated by

$$k_{//}(\sigma) = 2Z_0 \int i_0(t)(i_0(t) - i_m(t)) dt / \left[\int i_0(t) dt \right]^2, \quad (5)$$

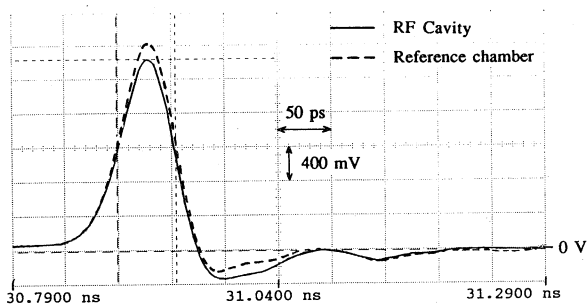


Fig. 6 Recorded output pulses $I_0(t)$ for the reference pipe and $I_m(t)$ for the RF cavity.

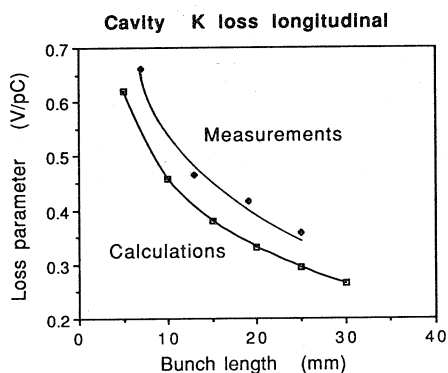


Fig. 7 Loss parameters of the RF cavity for measurements and numerical simulations.

where Z_0 is the characteristic impedance of the coaxial line formed by the reference chamber with wire and σ the length of the Gaussian pulse. Figure 6 shows the recorded output pulses from both the reference chamber and an RF cavity with nose cones. The measured loss parameters are plotted in Fig. 7 together with the calculated results by TBCI. They were obtained for four pulse widths; about 50, 100, 150, and 200 ps. The measurement data look somewhat overestimated, but both measurement and calculation show the same distribution property. The causes of overestimation are considered such that the generated pulse didn't have a perfect Gaussian distribution and the coaxial line in the tapered chamber didn't match well with the 50 Ω cable and connectors.

Measurement method has its drawbacks: the first is the measurement precision and the second is that the objects are limited in number. In the next step, we improve the measurement precision and then measure the loss parameters of a vacuum chamber with antechamber, a Conflat flange, and RF contact.

Conclusion

The impedances of vacuum chamber components turns out to be serious problem in our storage ring. A special attention has to be paid on the design of each component in order to achieve the designed performance. The most critical elements have been found to be transitions to ID chambers, flanges, and RF cavities. However, the transitions to ID chambers are, in fact, tapered smoothly and the impedance gets small. On the other hand, the impedance of bellows can be reduced sufficiently by screening them with RF contacts.

We have estimated the impedance in three ways: analytical calculation, numerical simulation, and measurement. The analytical calculation is only preliminary and limited to simple geometries. The numerical simulation and measurement also have many limitations. We need to estimate almost all the vacuum components of the storage ring by using three ways. From now on, we have to advance the calculation efficiency and have a plan to employ a 3D code, MAFIA. We also have to improve the measurement precision and estimate the other vacuum components: a crotch, gate valve, and so on.

References

1. E. Keil and W. Schnell, CERN-ISR-TH-RF/69-48, 1969.
2. A. G. Ruggiero, BNL Informal Report, Aug. 1979.
3. T. Weiland, Nucl. Inst. Meth. 212, 1983.
4. R. Klatt, et al., Proceeding of the 1986 Linear Accelerator Conference, SLAC, 1986.
5. B. Zotter, CERN LEP-TH/87-34, 1987.
6. T. Kusaka, et al., presented at this symposium.
7. M. Sands and J. Rees, SLAC-report PEP-95, 1974.